厚生労働科学研究費補助金

エイズ対策研究事業

エイズ多剤併用療法中のリザーバーの特定および選択的障害に関する研究

平成２１年度　総括研究報告書

研究代表者　五十嵐　樹彦

平成２２（２０１０）年　４月

目　　次

I. 厚生労働科学研究費補助金（エイズ・肝炎・新興再興感染症研究事業）
（総括・分担）研究報告書

エイズ多剤併用療法中のリザーバーの特定および選択的障害に関する研究

研究代表者　五十嵐　樹彦　京都大学ウイルス研究所教授

研究要旨

サルエイズモデルを用いて多剤併用療法中もウイルスを保持し続けるリザーバーを同定する目的で、今年度は２０年度に確立した強力な抗ウイルス多剤併用療法をSIV感染サルに適用し、投薬中止直後に安楽殺、全身の主要組織中のウイルスRNA量を定量した。その結果、治療個体の非リンパ系組織、中枢神経系及び感染急性期に劇的なリンパ球減少が起こる腸管等のエフェクターサイトにおけるウイルスRNA量は治療個体では検出限界以下であった。これに対して検索した全てのリンパ系組織からウイルスRNAが検出され、それらは非治療個体の1/1000 – 1/10000であった。以上の結果を元にリンパ組織から調整した組織切片を免疫組織化学染色した所、非常に低い頻度ながら、ウイルスタンパク(Nef)陽性細胞が検出された。以上の研究結果より、多剤併用療法下においてウイルスリザーバーはエフェクターサイトではなく、リンパ系組織及びそこに存在する細胞である事が強く示唆された。

A. 研究目的

抗 HIV-1 多剤併用療法の確立により、HIV-1 感染症は死に至る病ではなくなったが、この療法は未だ完全なものではなく、問題も認識されている。多剤併用療法の根本的な問題は感染者からウイルスを完全に排除する事が出来ない点であり、この為、感染者は薬剤を一生服用せねばならず、薬剤の副作用、変異ウイルスの出現、高額な医療費等の問題が派生する。本研究計画では多剤併用療法中にウイルスを保持し続けるリザーバーを特定、そのリザーバーを選択的に傷害する方法の開発を最終目的とする。リザーバーの全身レベルでの検索を行う為、サルエイズモデルであるSIVmac/アカゲザル実験系を用いることとした。このモデル系においてリザーバーの検索に応用できる様な強力な化学療法は 20 年度に既に確立した。21 年度は感染サルに確立した多剤併用療法を適用、投薬中止直後に安楽殺し各組織を RT-PCR 及び免疫組織化学により検索した。

B. 研究方法

20 年度に確立した多剤併用療法は以下の通りである。逆転写阻害剤としてジドブジン(AZT)、ラミブジン（3TC）、テノフォビル（TDF）を選択した。プロテアーゼ阻害剤としてロピナビル(LPV)およびリトナビル(RTV)を選択した。投薬は選択した抗ウイルス剤（市販、成人感染者推奨服薬量の半量）を粉砕、同じく粉砕したサル飼料（PMI 社製 Certified animal diet 5048）30 グラムとバナナ 75 グラムを混合、成形し、1 日2回(TDF のみ 1 日 1 回)、10 時間および 14 時間

間隔で自由摂食させた。ウイルスは病原性SIVmac239を2000 $TCID_{50}$静脈内接種した。サルは中国産アカゲザル3頭を用い、1頭は非治療対照とし、2頭に多剤併用療法を感染8週後から10週間及び38週後から8週間適用した。2度目の投薬を中止して10日後、治療個体を安楽殺し、全身のリンパ系組織及び主要組織を採材した。各組織は、組織学的検索用に10%中性ホルマリンで固定後、包埋・薄切した。組織切片はSIV Nef特異的単クローン抗体を反応させ、ウイルス感染細胞を検出した。また、RNA安定化溶液に浸漬後、凍結保存した各組織より総RNAを抽出し、SIV gag特異的プライマー/プローブを用いリアルタイムPCRにより遺伝子の増幅・定量を行った。エイズ期のSIV感染非治療個体から上記に準じ組織を採取、対照とした。ウイルス接種後、経時的に採取した血液から血漿を調整、ウイルスRNA量をPCRにより定量した。

（倫理面への配慮）

実験は「研究機関等における動物実験等の実施に関する基本指針」に基づく「京都大学における動物実験の実施に関する規定」を遵守し行った。

C. 研究結果

1. SIV感染アカゲザルの血漿中ウイルスRNA量への多剤併用療法の効果

3頭のアカゲザルにSIV239を静脈内接種し、血漿中ウイルスRNA量を定量し検索した。全てのサルで接種2週後に7×10^6–6×10^7コピー/mlのピークに達し、その後、接種5週後から1.5–5×10^5コピー/mlで安定した。そこで接種8週後から10週間、2頭に対して多剤併用療法を適用した。非治療個体ではこの間、3×10^5コピー/mlから5×10^4コピー/mlに漸減した。治療個体では治療開始後4週間以内に2.6×10^5および3×10^5コピー/mlだった血漿ウイルスRNA量が、検出限界である200コピー/ml未満に抑制された。治療開始10週後（ウイルス接種18週後）に投薬を中止すると、3–4週間以内に血漿中ウイルス量は非治療個体と同水準の10^4コピー/mlに上昇した。その後、治療経験個体の血漿中ウイルス量は非治療個体と同様漸増し、接種38週後に3.8及び8.6×10^4コピー/mlに達した。再び治療経験個体に1回目と同一の多剤併用療法を適用した所、1頭では治療開始1週間以内に、もう1頭では5週間以内に検出限界未満に低下し、投薬期間中血漿中ウイルスRNAは検出されなかった。治療開始8週後（ウイルス接種46週後）に投薬を中止し、その10日後に治療経験個体を安楽殺した。この時の血漿中ウイルスRNA量は1頭で検出限界以下、もう1頭で1.4×10^3コピー/mlであった。

2. 各組織におけるウイルスRNA量

治療個体の非リンパ系主要臓器（心、肝、腎、膵）のウイルスRNA量は検出限界以下であった。薬剤投与されていないSIV239感染アカゲザルにおいてはこれら臓器で1.3–4.4×10^5コピー/μg総RNAのウイルスRNAが検出された。

HIV-1およびSIV感染急性期には、腸管等のエフェクターメモリーT細胞が多く存在す

る、所謂「エフェクターサイト」でウイルスが爆発的に複製し、リンパ球を著減させる事が知られている。非治療個体の膣、直腸及び空腸からそれぞれ 3.2×10^5、1.2×10^6、9.9×10^7 コピー/μg 総 RNA のウイルス RNA が検出されたが、治療経験個体のこれら組織におけるウイルス RNA 量はいずれも検出限界以下であった。

中枢神経系は現行の抗 HIV-1 剤が到達せず、ウイルスの聖域と考えられている。解析を行ったエイズ期 SIV 感染非治療個体では中枢神経系ウイルス RNA 量は大脳、小脳、脳幹においてそれぞれ 2.6、3.9、3.7×10^4 コピー/μg 総 RNA であったが、治療経験個体では安楽殺時血漿中ウイルス RNA 量が検出限界以下であった個体では、全て検出限界以下、血漿中RNA量が 1.4×10^3 コピー/ml であった個体では大脳及び小脳で検出限界以下、脳幹で 1.4×10^3 コピー/μg 総 RNA であった。

HIV-1 および SIV はリンパ球指向性である事から、リンパ系組織は非治療個体においてはウイルス量が多い。そこでこの組織における多剤併用療法のウイルス抑制効果を解析した。非治療個体では $5.6\text{-}9.2\times10^8$ コピー/μg 総 RNA と非常に高いウイルス量が検出された。治療経験個体では、これより低いものの、検索したほぼ全てのリンパ系組織でウイルス RNA が検出された。安楽殺時の血中ウイルス量が 1.4×10^3 コピー/ml だった個体では 3.5×10^5–1.6×10^6 コピー/μg 総 RNA、血中ウイルス量が検出以下だった個体でも 2×10^3–4×10^5 コピー/μg 総 RNA のウイルス RNA を保有していた。

3. リンパ系組織における感染細胞の検出

PCR 検索から治療中止直後の個体ではリンパ系組織でウイルス RNA が検出されたため、この組織に絞ってウイルス感染細胞の免疫組織化学による検出を試みた。感染細胞において大量の発現が見られる Nef タンパクを指標に免疫組織化学を実施した。治療経験個体の両方で Nef 陽性細胞が検出された。陽性細胞は非常に低い出現頻度ながら胚中心及び傍皮質領域で検出された。

D.考察

今年度の成果で最も重要なものは、多剤併用療法中止直後にリンパ系組織でウイルス複製が見られた事である。活発なウイルス複製及びそれによる細胞傷害の起こる場として、「エフェクターサイト」が認められているが、今回の解析結果からは、「エフェクターサイト」はウイルスリザーバーとならないと考えられる。「エフェクターサイト」は抗ウイルス剤が浸透しやすく、リンパ系組織には浸透しにくい可能性は、リンパ系は解放系で血液・脳関門の様な障壁が存在しない事から考えにくい。むしろ、多剤併用療法中もウイルスを産生し続ける細胞の頻度が「エフェクターサイト」では少なく、リンパ系組織では多いと考えられる。

リンパ系組織のどの細胞がウイルスリザーバーとして機能しているかは、現在、多重免疫染色及びin situ hybridization/免疫組織化学複合染色により検索中である。すでにリザーバーとして確立されたメモリーCD4陽性T細胞の他にウイルス産生細胞が存在するかはリザーバーの選択的傷害を考える際大変重要

な問題であるので、拙速にならないよう慎重に検索を進めたい。

今回の検索に用いたSIV239/アカゲザルエイズモデルは現在、最も広く用いられているエイズ動物モデルであるが、

1.ウイルスが分子クローンである事、

2. T細胞指向性である事から、実際のHIV-1感染を再現していない可能性がある事も忘れてはならない。

E.結論

SIV239/アカゲザルエイズモデルにおいて多剤併用療法中にリンパ系組織及びそこに存在する細胞がウイルスリザーバーとなる事が示唆された。

F.健康危険情報

なし

G.研究発表

1.論文発表

- Nishimura, Y., Sadjadpour, R., Mattapallil, J.J., Igarashi, T., Lee, W., Buckler-White, A., Roederer, M., Chun, T.W., and Martin, M. A. (2009) High frequencies of resting CD4+ T cells containing integrated viral DNA are found in rhesus macaques during acute lentivirus infections. Proc. Natl. Acad. Sci. USA 106: 8015-8020.

- Kubo, M., Nishimura, Y., Shingai, M., Lee, W., Brenchley, J., Lafont, B., Buckler-White, A., Igarashi, T., and Martin, M.A. (2009) Initiation of antiretroviral therapy 48 hours after infection with simian immunodeficiency virus potently suppresses acute-phase viremia and blocks the massive loss of memory CD4+ T cells but fails to prevent disease. J. Virol., 83: 7099-7108.

- Suzuki, T., Yamamoto, N., Nonaka, M., Hashimoto, Y., Matsuda, G., Takeshima, S. N., Matsuyama, M., Igarashi, T., Miura, T., Tanaka, R., Kato, S., and Aida, Y. (2009) Inhibition of human immunodeficiency virus type 1 (HIV-1) nuclear import via Vpr-Importin alpha interactions as a novel HIV-1 therapy. Biochem. Biophys. Res. Commun., 380: 838-843.

2.学会発表

- 松田健太、稲葉一寿、伊吹謙太郎、深澤嘉伯、松山めぐみ、斉藤尚紀、堀池麻里子、姫野愛、速水正憲、五十嵐樹彦、三浦智行：新規CCR5指向性SHIVの作製とアカゲザルへの順化、第148回日本獣医学会学術集会、2009年9月25-27日、鳥取

- 松田健太、稲葉一寿、深澤嘉伯、伊吹謙太郎、松山めぐみ、堀池麻里子、速水正憲、五十嵐樹彦、三浦智行：抗HIVワクチン評価に有用なR5指向性SHIVの作製、第57回日本ウイルス学会学術集会、2009年10月25-27日、東京

高原悠佑、武内寛明、石井洋、高橋尚史、三浦智行、五十嵐樹彦、俣野哲朗：ビルマ産アカゲザルSIV感染により誘導されるCTLエピトープの探索、第57回日本ウイルス学会学術集会、2009年10月25-27日、東京

H.知的財産権の出願・登録状況（予定を含む）

なし

II. 研究成果の刊行に関する一覧表

書籍　なし

雑誌

発表者氏名	論文タイトル名	発表誌名	巻号	ページ	出版年
Nishimura, Y., Sadjadpour, R., Mattapallil, J.J., Igarashi, T., Lee, W., Buckler-White, A., Roederer, M., Chun, T.W., Martin, M. A.	High frequencies of resting CD4+ T cells containing integrated viral DNA are found in rhesus macaques during acute lentivirus infections.	Proceedings of the National Academy of Sciences of the United States of America	106	8015-8020	2009
Kubo, M., Nishimura, Y., Shingai, M., Lee, W., Brenchley, J., Lafont, B., Buckler-White, A., Igarashi, T., Martin, M.A.	Initiation of antiretroviral therapy 48 hours after infection with simian immunodeficiency virus potently suppresses acute-phase viremia and blocks the massive loss of memory CD4+ T cells but fails to prevent disease.	The Journal of Virology	83	7099-7108	2009

Suzuki, T., Yamamoto, N., Nonaka, M., Hashimoto, Y., Matsuda, G., Takeshima, S. N., Matsuyama, M., Igarashi, T., Miura, T., Tanaka, R., Kato, S., Aida, Y.	Inhibition of human immunodeficiency virus type 1 (HIV-1) nuclear import via Vpr-Importin alpha interactions as a novel HIV-1 therapy.	Biochemical and Biophysical Research Communications	380	838-843	2009

III. 研究成果の刊行物・別刷

High frequencies of resting CD4$^+$ T cells containing integrated viral DNA are found in rhesus macaques during acute lentivirus infections

Yoshiaki Nishimura[a], Reza Sadjadpour[a], Joseph J. Mattapallil[b,1], Tatsuhiko Igarashi[a], Wendy Lee[a], Alicia Buckler-White[a], Mario Roederer[b], Tae-Wook Chun[c], and Malcolm A. Martin[a,2]

[a]Laboratory of Molecular Microbiology, [b]Vaccine Research Center, and [c]Laboratory of Immunoregulation, National Institute of Allergy and Infectious Diseases, National Institutes of Health, Bethesda, MD 20892

Contributed by Malcolm A. Martin, March 23, 2009 (sent for review March 2, 2009)

We and others have reported that the vast majority of virus-producing CD4$^+$ T cells during the acute infection of rhesus macaques with simian immunodeficiency virus (SIV) or CXCR4 (X4)-using simian/human immunodeficiency viruses (SHIVs) exhibited a nonactivated phenotype. These findings have been extended to show that resting CD4$^+$ T lymphocytes collected from SIV- or X4-SHIV-infected animals during the first 10 days of infection continue to release virus ex vivo. Furthermore, we observed high frequencies of integrated viral DNA (up to 5.1 × 10^4 DNA copies per 10^5 cells) in circulating resting CD4$^+$ T cells during the first 10 days of the infection. Integration of SIV DNA was detected only in memory CD4$^+$ T cells and SHIVs preferentially integrated into resting naïve CD4$^+$ T cells. Taken together, these results show that during the acute infection large numbers of resting CD4$^+$ T cells carry integrated nonhuman primate lentiviral DNA and are the major source of progeny virions irrespective of coreceptor usage. Prompt and sustained interventions are therefore required to block the rapid systemic dissemination of virus and prevent an otherwise fatal clinical outcome.

HIV | integration | simian immunodeficiency virus | simian/human immunodeficiency virus

During the first 15 years of the AIDS epidemic, the prevailing dogma was that HIV and simian immunodeficiency virus (SIV) were unable to replicate in quiescent CD4$^+$ T lymphocytes (1, 2). This failure to infect nonactivated T cells in culture was attributed to multiple mechanisms including inefficient reverse transcription (RT) (1, 3–5), impaired nuclear import of reverse transcripts (6, 7), and low intracellular dNTP pools (8). It was also believed that HIV was unable to integrate into the genome of resting CD4$^+$ T cells (9). Because unintegrated DNA has been reported to be inefficiently transcribed (10–12), impaired integration could also contribute to the failure of lymphocytes in the $G_{0/1a}$ stage of the cell cycle to support productive infections (13).

Although these results have been confirmed in numerous laboratories, studies conducted during the past decade have shown that resting T cells, recovered from human lymphoid tissue explants maintained ex vivo, release substantial quantities of progeny virions (14, 15). Another report demonstrated that resting CD4$^+$ T lymphocytes, in specimens obtained from HIV-infected individuals or acutely SIV-infected macaques, are producing viral RNA (16). We reported that 32–88% of circulating naïve CD4$^+$ T lymphocytes from rhesus monkeys infected with CXCR4-tropic (X4-tropic) simian/human immunodeficiency viruses (SHIVs) were productively infected by day 10 postinfection (PI) (17). Immunophenotyping by flow cytometry and combined in situ hybridization/immunohistochemistry revealed that the vast majority of the virus-producing CD4$^+$ T lymphocytes collected from these SHIV-infected animals were not expressing activation markers.

It could be argued that the prodigious levels of virus production by quiescent naïve cells measured by endpoint dilution/cocultivation reflected the activating effects induced by the monoclonal antibodies used for positive cell sorting and/or the subsequent incubation with MT4 cells (17). Accordingly, negatively-selected resting CD4$^+$ T lymphocytes were purified from SIV-infected (day 7 PI) and SHIV-infected (day 10 PI) rhesus monkeys and cultivated in the presence of autologous serum and the absence of IL-2 for 4 days. Infectious virus was, in fact, detected in the supernatant medium from each ex vivo culture. In a separate series of experiments, the integration status of viral DNA in resting naïve and memory CD4$^+$ T cells, recovered from SIV- and SHIV-infected macaques on days 7 and 10 PI, respectively, was determined by limiting dilution Alu-LTR PCR. High frequencies of integrated SIV DNA were detected in memory but not naïve CD4$^+$ T cells, in agreement with the differential expression of the CCR5 coreceptor in these 2 lymphocyte subsets (18, 19). In animals inoculated with X4-tropic SHIV, 13–51% of the circulating naïve CD4$^+$ T cells contained integrated DNA, assuming each cell carries a single integrated provirus. These results indicate that during the acute infection, integration of viral DNA occurs in a prototypical resting cell.

Results

In earlier experiments evaluating virus production during the acute infection of 3 rhesus monkeys with the highly-pathogenic X4-tropic $SHIV_{DH12R}$, we reported that resting naïve CD4$^+$ T cells were massively infected and, as shown in Fig. 1, were the major source of infectious virus circulating in the blood on day 10 PI (17). In that study, activated CD8$^+$ T lymphocytes were observed in the blood (CD69$^+$, HLA-DR$^+$, and Ki-67$^+$) and lymph nodes (Ki-67$^+$) by week 2 PI, but the activation status of CD4$^+$ T cells recovered from these sites remained unchanged from their preinoculation resting state. Confocal microscopy of day 10 lymph node specimens, using SIV riboprobes and the anti-Ki-67 mAb, revealed that >96% of SHIV-producing cells did not express Ki-67. Taken together, these results indicated that the vast majority of virus-producing cells during the acute in vivo infection exhibited a nonactivated phenotype.

As a follow-up to this initial study, we wanted to answer 2 questions: (*i*) would virus production by resting CD4$^+$ T lymphocytes, after their isolation from acutely infected animals, continue ex vivo and (*ii*) what was the integration status of viral DNA in resting virus-producing CD4$^+$ T cells in vivo? Accordingly, individual rhesus monkeys were inoculated intravenously

Author contributions: Y.N., T.I., T.-W.C., and M.A.M. designed research; Y.N., R.S., J.J.M., W.L., A.B.-W., and M.R. performed research; Y.N. and R.S. analyzed data; and Y.N. and M.A.M. wrote the paper.

The authors declare no conflict of interest.

[1]Present address: Department of Microbiology and Immunology, Uniformed Services University, Bethesda, MD 20814.

[2]To whom correspondence should be addressed. E-mail: malm@nih.gov.

This article contains supporting information online at www.pnas.org/cgi/content/full/0903022106/DCSupplemental.

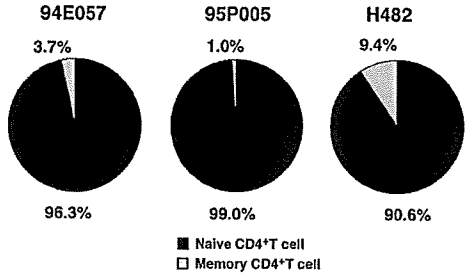

Fig. 1. Naive CD4+ T cell are the major source of infectious virus circulating in the blood during the acute infection of rhesus monkeys with $SHIV_{DH12R}$. The frequencies of productively-infected naïve or memory cells collected on day 10 PI from 3 $SHIV_{DH12R}$-infected animals were determined by cocultivation with MT4 cells for 14 days as described (17).

with 1×10^4 $TCID_{50}$ SIVmac239 (macaque CN30) or 1×10^5 $TCID_{50}$ $SHIV_{DH12R}$ (macaque WGG) and the levels of plasma viremia and circulating CD4+ T cells were determined during the first 10 days of infection (Fig. 2*A*). The SIV-infected animal experienced a more rapid increase of its plasma virus load compared with the SHIV-infected macaque and both monkeys sustained partial depletions of their peripheral blood CD4+ T cells. Peripheral blood mononuclear cells (PBMCs) were prepared from both monkeys on days 7 and 10 PI and a portion of each PBMC sample was sorted by FACS for quantitative cell-associated viral DNA content in naive ($CD95^{low}CD28^{high}$) or memory ($CD95^{high}CD28^{low\ and\ high}$) CD4+ T lymphocytes. As shown in Fig. 2*B*, high levels (3.1 or 3.8×10^4DNA copies per 10^5 cells) of memory CD4+ T cells from the SIV-infected macaque contained viral DNA on days 7 and 10 PI, whereas the frequency of infected naïve cells was significantly lower. This difference is consistent with the expression levels of the CCR5 coreceptor used by SIV in these 2 CD4+ T lymphocyte subsets. In contrast, $SHIV_{DH12R}$ DNA was detected in both naïve and memory CD4+ T cells, reaching levels of 1.6×10^4 and 1.7×10^4 DNA copies per 10^5 cells, respectively, on day 10 PI, consistent with the surface expression of CXCR4 on both CD4+ T cell subsets (20).

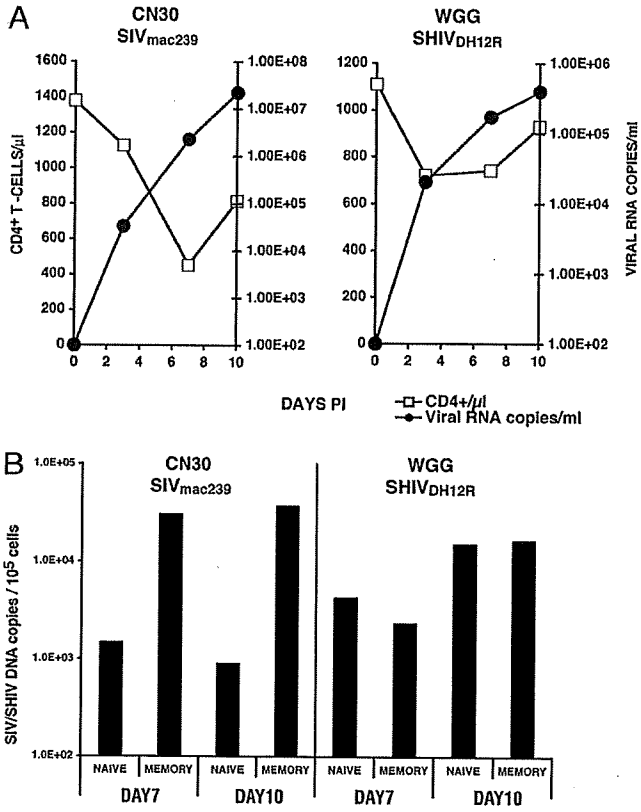

Fig. 2. Peripheral blood CD4+ T cell profiles and viral nucleic acid levels during the acute SIV and SHIV infections of macaques. (*A*) Circulating CD4+ T cell numbers and plasma viral RNA loads were measured in a SIV (CN30)-infected and a $SHIV_{DH12R}$ (WGG)-infected rhesus monkey at the indicated times. (*B*) PBMC samples, collected on days 7 and 10 PI from macaques CN30 and WGG, were stained with anti-CD3, CD4, CD28, and CD95 mAbs to distinguish naïve from memory CD4+ T cells and sorted by FACS for determinations of the cell-associated viral DNA copies per 10^5 cells by DNA PCR.

Spontaneous Virus Production by Resting CD4+ T Cells ex Vivo. To preserve the nonactivated status of CD4+ T cells during purification, PBMC samples, collected on day 7 from SIV-inoculated macaque CN30 and on day 10 from SHIV-inoculated macaque WGG, were initially stained with non-CD4+ T cell markers (CD8, CD20, CD14, and CD16) and markers of activation (CD25, CD69, and HLA-DR). These collection times were selected because: (*i*) circulating memory CD4+ T lymphocytes had declined to low levels in the SIV-infected monkey (CN30) by day 10 PI; and (*ii*) larger numbers of $SHIV_{DH12R}$-infected cells were present in animal WGG on day 10 compared with day 7 PI. Lymphocytes, negative for non-CD4 and activation markers, were then sorted by FACS. The purity of the resulting CD4+ T cell populations from both animals was >96%; these cells expressed minimal levels of CD25, CD69, or HLA-DR (Fig. 3*A*).

The negatively-sorted resting CD4+ T cell preparation from each animal was cultured in duplicate for 4 days in the absence of any stimulation, including exogenous IL-2, as described in *Methods*. The production of progeny virus was monitored daily by measuring RT activity released into the medium. No RT activity was measured in these culture supernatants. The detection limit of the ^{32}P-RT-assay used (21) ranged from 2.5×10^3 to 8×10^3 $TCID_{50}$/mL, based on RT measurements of SIV and SHIV stocks of known infectious titer. To amplify any infectious virus released into the medium, filtered supernatants, collected daily (days 1–4) from the RT-negative duplicate cultures of resting SIV- or SHIV-infected CD4+ T cells, were spinoculated onto MT-4 T cells, and the duplicate cultures of MT-4 T cells were maintained for an additional 14 days. As shown in Fig. 3*B*, RT activity was detected as early as day 1 (1 of 2 wells) in the supernatants from each of the original nonactivated CD4+ T cell cultures. Both duplicate wells were positive for SIV and SHIV production in supernatants collected on days 3–4. These results indicate that resting CD4+ T cells, collected from macaques during acute SIV and SHIV infections, continued to produce and release progeny virions during 4 days of ex vivo cultivation.

Integration Status of Viral DNA in CD4+ T Lymphocytes During Acute SIV and SHIV Infections. Because of the long-standing belief that integration of reverse transcripts did not occur in quiescent cells, we next investigated whether integrated DNA could be detected during the primary infection. A modified Alu-LTR PCR approach, using pairs of outward-facing PCR primers binding to conserved regions of human and rhesus macaque AluDNA sequences, in conjunction with a cloned cell line containing a single copy of integrated SIV DNA, were used to analyze genomic DNA prepared from sorted and endpoint-diluted naïve and memory CD4+ T cells from acutely SIV- and SHIV-infected animals.

The 3D8 cell line, carrying 1 copy of integrated SIV DNA, was derived from chronically-infected CEM×174 cells, 8 weeks after infection with SIVmac316, as described in *SI Text*. Cells carrying viral DNA were initially identified by DNA PCR and then

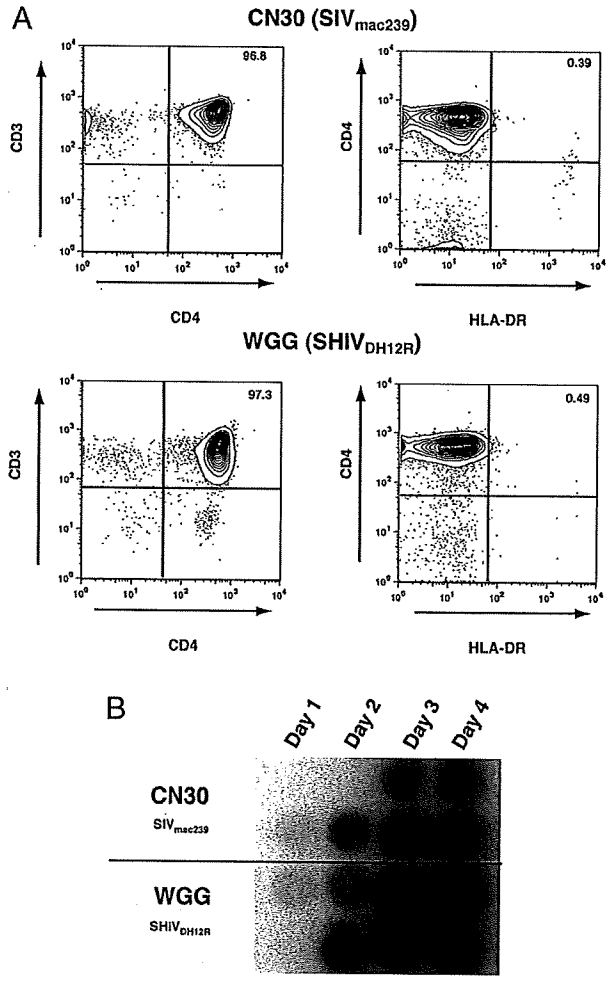

Fig. 3. Resting CD4+ T cells from acutely SIV and SHIV-infected macaques continue to release progeny virions ex vivo. (*A*) Nonactivated CD4+ T cells were purified by negative FACS sorting from PBMCs collected on day 7 from macaque CN30 (SIV_{mac239}) or day 10 from macaque WGG ($SHIV_{DH12R}$) as described in *Methods*. The FACS profiles of CD4+ HLA-DR+ cells from each monkey are shown. (*B*) Purified resting CD4+ T cells were treated with Pronase to eliminate any surface-bound virions and cultured for 4 days in the absence of any stimulation in RPMI medium 1640 supplemented with 15% autologous serum. Culture supernatants were collected daily, filtered, and spinoculated on MT-4 T cells, in duplicate, to amplify low levels of released progeny virions. Virus production was assessed by measuring the 32P-RT activity released into the medium of duplicate MT-4 cultures on day 14 PI by autoradiography.

examined by Southern blot analysis to ascertain SIV proviral DNA copy number, using EcoRI, BamHI, and SacI, which cleave SIVmac316 DNA 0, 1, and 2 times, respectively. An analysis of 3D8 cellular DNA, carried out in triplicate and shown in Fig. S1, is consistent with the presence of a single integrated copy of SIV DNA in this cloned line.

Limiting dilution Alu-LTR PCR, performed on specimens recovered from acutely-infected macaques, was used to quantitate the frequency of integrated viral DNA. The values obtained from these samples were then compared with those derived from 3D8 cells, which were contemporaneously examined. A representative analysis of 3D8 cellular DNA performed in triplicate is shown in Fig. 4*A*. The mean number of cells required to detect the single copy of SIV DNA in this cell line was 3.3, based on several independent experiments. This level of sensitivity is similar to that reported for the ACH-2 cell line, which also contains a single copy of integrated HIV-1 DNA (22).

Genomic DNAs, prepared from positively-sorted naïve or memory CD4+ T cells on day 7 PI from the SIV (CN30), day 10 PI from the SHIV (WGG)-infected macaque, or day 10 PI from the 3 previously-studied SHIV-infected animals (94E057, 95P005, and H482) shown in Fig. 1, were endpoint-diluted and evaluated by Alu-LTR PCR. A representative analysis of the integrated SHIV DNA present in CD4+ T lymphocytes from monkey 95P005 is shown in Fig. 4*B*. Because a mean of 3.3 3D8 cells was required to detect the single copy of SIV DNA present per cell, the values obtained from the naïve or memory cells, recovered from SHIV/SIV-infected animals, were normalized accordingly. Based on this determination, the number of naïve CD4+ T cells needed to amplify a single copy of integrated DNA from macaque 95P005 was 2.0 cells; the number of memory CD4+ T cells required was higher (7.9 cells). As shown in Fig. 4*C* and Table S1, 2.0–7.9 naïve CD4+ T lymphocytes collected from the 4 SHIV-infected monkeys on day 10 PI were required to detect integrated proviral DNA. Thus, the frequency of integrated SHIV DNA in circulating naive CD4 T cells was surprisingly high, ranging from 1.27 to 5.08×10^4 DNA copies per 10^5 cells, with a mean of 2.43×10^4 DNA copies per 10^5 cells. The numbers of memory CD4+ T cells from these 4 animals needed to amplify a single copy of integrated viral DNA were higher (7.9–15.8 cells). The frequency of integrated SHIV DNA in memory CD4+ T cells ranged from 6.34×10^3 to 1.27×10^4 DNA copies per 10^5 cells with a mean 1.01×10^4 DNA copies per 10^5 cells.

In the single SIV-infected animal (CN30) evaluated, the number of memory CD4+ T cell needed to amplify a single copy of integrated DNA and the frequency of integrated viral DNA were 15.8 cells and 6.34×10^3 DNA copies per 10^5 cells, respectively, for samples collected on day 7 PI (Fig. 4*C* and Table S1). As expected from its coreceptor usage, integrated SIV DNA was undetectable in naïve CD4+ T cells (even when >500 cells were analyzed per reaction).

The total cell-associated viral DNA in naïve or memory CD4+ T cells recovered from each animal was measured by quantitative DNA PCR using SIV *gag* primers (Table 1). Although the different PCR assay systems used to quantitate integrated and total SIV and SHIV DNAs in the CD4+ T cells subsets make direct comparisons of viral DNA frequencies problematic, higher levels of total viral DNA were generally measured. Nonetheless, the frequencies of viral DNA copies per 10^5 cells measured were very high in both assays.

Discussion

Activated PBMC cultures or T cell leukemia cell lines have been used for >20 years to study HIV replication and spreading infections in vitro. It has been assumed by many that the replicative properties of diverse HIV-1 strains, measured in these in vitro systems, are reflective of virus infectivity in vivo. However, most CD4+ T lymphocytes in vivo are not activated and those that are may not reach the levels of activation achievable in vitro. As noted earlier, resting PBMC cultures or purified quiescent CD4+ T lymphocyte preparations are resistant to HIV-1 infection in vitro. This resistance has been ascribed to a generalized impairment/inefficiency of several critical steps in the virus life cycle including entry, RT, and nuclear import. Although it was once thought that the integration reaction is blocked in nonactivated CD4+ T cells, at least 3 recent studies (23–25) report that HIV-1 DNA integrates into the chromosomal DNA of resting cells, even when the size of the virus inoculum is low. Nonetheless, spontaneous release of progeny virions in these systems has never been observed, but can be induced after treatment with anti-CD3 plus anti-CD28 mAbs (24).

We and others have reported that during the acute infection of rhesus macaques with either SIV or X4-SHIVs, most virus-

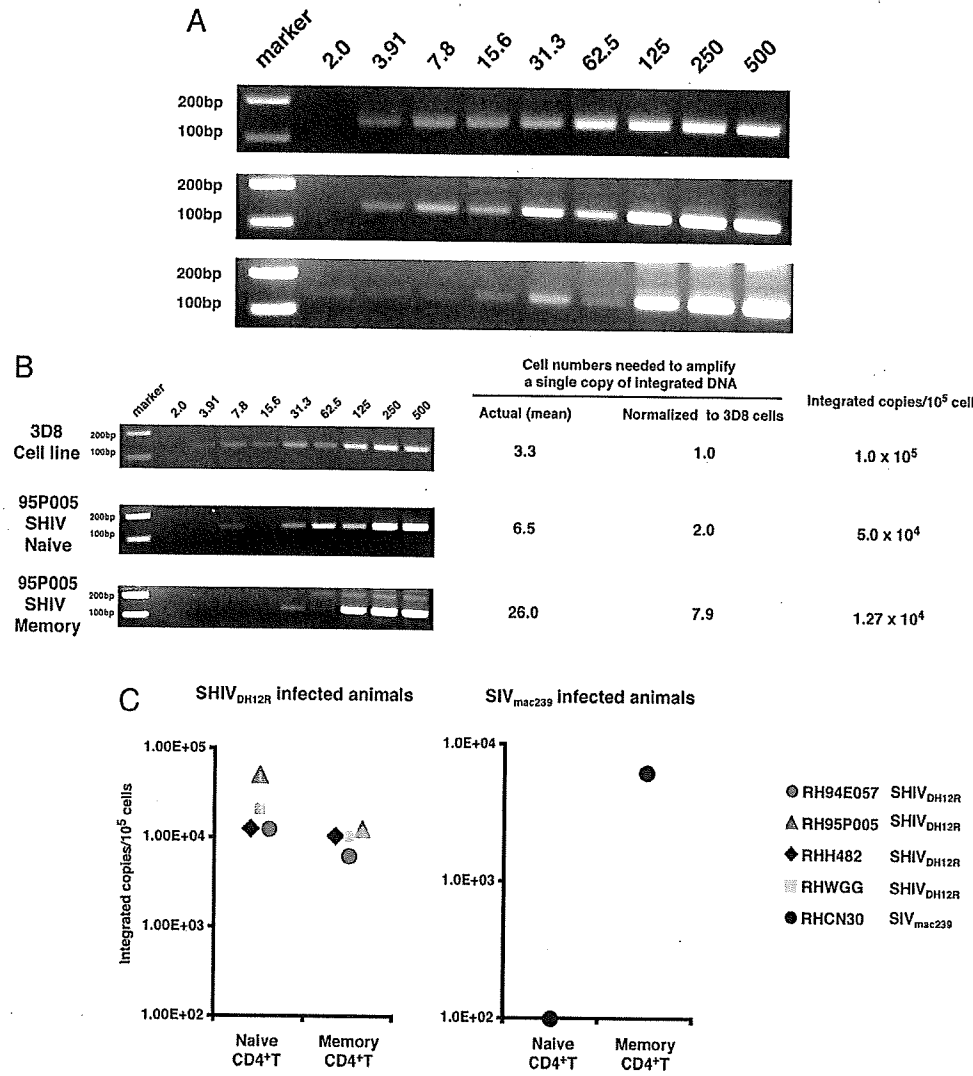

Fig. 4. Quantitation of integrated viral DNA in naïve or memory CD4+ T cells collected from acutely SIV or SHIV-infected macaques. (*A*) Genomic DNA from 3D8 cells was serially diluted 2-fold, in triplicate, starting with 500 cell DNA equivalents and analyzed by Alu-LTR PCR. (*B*) Genomic DNAs, purified from sorted naïve or memory CD4+ T cells from $SHIV_{DH12R}$-infected macaque 95P005 on day 10 PI, were serially diluted, and integrated proviral DNA was measured by Alu-LTR PCR. (*C*) The frequencies of naïve or memory CD4+ T cells carrying integrated SIV or SHIV DNA were determined by Alu-LTR PCR and normalized to the values obtained with the 3D8 cell line.

infected cells were immunophenotypically resting memory and naïve CD4+ T lymphocytes, respectively (16, 17, 26). We have extended this observation in the current study and found that nonactivated virus-infected cells, recovered from acutely-infected animals, continue to release low levels of infectious progeny virions ex vivo without additional stimulation. In this regard, intriguing quantitative differences have been reported when HIV-1 RT and integration reactions are evaluated during ex vivo infections of CD4+ T cells exhibiting a continuum of activation states. For example, when viral DNA generated by RT is measured in ex vivo-activated versus freshly-purified resting T cells, 30- to 100-fold more DNA copies per cell are detected in the former (24, 25). In contrast, the HIV-1 DNA content in "endogenously" activated CD4+ T cells (negatively-sorted CD4+ T lymphocytes expressing HLA-DR and CD69) was only 2-fold higher than that present in resting T cells. A similar hierarchy of relative integration frequencies (1:5:50) was observed for resting, endogenously-activated, and ex vivo-activated CD4+ T cells, respectively. These results suggest that virus infectivity in vivo, both in resting and activated CD4+ T cells, may be far less robust than that measured in vitro.

HIV-infected resting CD4+ T cells have been identified during both the acute and chronic phases of infection in vivo. Some reports (27, 28) have described the presence of integrated HIV-1 DNA and the recovery of virus from CD45RA+ naïve CD4+ T lymphocytes from chronically-infected individuals, particularly after coreceptor switching. In addition, latently HIV-1-infected, resting memory CD4+ T cells have been detected in individuals receiving highly active antiretroviral therapy with extremely low levels of viremia (29–31). When resting memory CD4+ T lymphocytes from viremic and nonviremic, latently-infected individuals were purified and cultured ex vivo in the absence of activating stimuli, only cells from viremic persons spontaneously released progeny virions (32).

In contrast to the chronic phase of the HIV-1 infection in which the frequency of latently-infected resting memory CD4+ T cells with replication competent-integrated provirus is exceedingly low (33), high levels of virus-producing resting cells have

Table 1. Frequencies of integrated and total viral DNA in naïve or memory CD4+ T cells in SHIV-infected (day 10) or SIV-infected (day 7) animals

Animal ID	CD4 subset	Integrated copies/ 10^5 cells	Total DNA copies/ 10^5 cells	Integrated/ total DNA ratio
94E057 (SHIV)	Naïve	1.27×10^4	7.25×10^4	0.17
	Memory	6.34×10^3	2.35×10^4	0.27
95P005 (SHIV)	Naïve	5.08×10^4	2.84×10^5	0.18
	Memory	1.27×10^4	1.07×10^5	0.12
H482 (SHIV)	Naïve	1.27×10^4	6.44×10^4	0.20
	Memory	1.06×10^4	5.67×10^4	0.19
WGG (SHIV)	Naïve	2.11×10^4	1.57×10^4	1.35
	Memory	1.06×10^4	1.71×10^4	0.62
CN30 (SIV)	Naïve	*	1.51×10^3	*
	Memory	6.34×10^3	3.13×10^4	0.20

*Below detection limit.

been reported during the acute infection. One study (16), using in situ hybridization in combination with staining by antibodies to activation and cell cycle markers, reported that 50% of the virus-infected cells in lymph node specimens from recently-infected individuals were HLA-DR$^-$ and KI-67$^-$, the resting memory subset. In the more tractable SIV/macaque system, a majority of virus-positive cells in lymph node biopsies were shown to be HLA-DR$^-$ and KI-67$^-$ on day 12 after intravaginal inoculation. Not unexpectedly, the intracellular levels of viral RNA measured in these experiments were 4- to 6-fold higher in activated cells present in the same microscopic fields. In a follow-up study using the same approach, >90% of SIV RNA-positive memory CD4+ T cells in the colon were found to be negative for CD69, CD25, and Ki-67 on day 10 PI (26).

In this study we have shown that both SIV and SHIVs are able to infect resting CD4+ T lymphocytes during the acute infection of rhesus monkeys and integrate DNA copies of their genomes into host cell chromosomal DNA. The observed high frequencies of resting CD4+ T cells carrying integrated viral DNA on day 7 PI (SIV) and day 10 PI (SHIV) is consistent with the reported high frequencies of virus-infected cells using other approaches (17, 34). In the case of acutely SHIV-infected macaques, 13–51% of the circulating naïve CD4+ T cells contained integrated viral DNA, which is in good agreement with the reported 30–90% frequency of naïve CD4+ T cells releasing progeny virions (17). The results of the integration assays also reflected the differential levels of coreceptor expression in the CD4+ T lymphocyte subsets targeted by SIV and X4-SHIVs (20). Integration of SIV DNA was observed only in memory CD4+ T cells and the X4 SHIVs preferentially integrated into naïve versus memory CD4+ T cells. Thus, during the acute infection of macaques, resting CD4+ T cells are the major targets of nonhuman primate lentiviruses, irrespective of their coreceptor usage.

Based on available evidence, the very low levels of virus production, observed in ex vivo cultures of resting CD4+ T cells from acutely SIV- and SHIV-infected monkeys (Fig. 3*B*), are difficult to reconcile with the high levels of plasma viremia ($\approx10^7$ RNA copies per mL) contemporaneously measured in these animals. A plausible explanation of this apparent paradox is that: (*i*) the high frequency of circulating infected, nonactivated CD4+ T lymphocytes is reflective of the extraordinarily large number of similar productively infected cells in lymphoid tissues and/or effector sites; (*ii*) the latter population produces small amounts of virus per cell; and (*iii*) the net effect of the slow release of small quantities of progeny virions by an enormous fraction of the total CD4+ T cell population would result in high SIV or SHIV virus loads, as suggested (26). In this regard, it has recently been reported that SIV-infected resting cells may generate 70–93% of peak virus production, based on Bayesian statistical analyses (35).

A related and currently-unresolved issue concerns the mechanism responsible for the prodigiously rapid rate of virus spread throughout a sizable fraction of total body CD4+ T cells during the initial weeks of the infection. It would seem unlikely that cell-free virus transmission alone could account for the rapid increase of virus-infected cells in vivo. The high concentrations of tightly-packed juxtaposed infected and uninfected resting CD4+ T cells in vivo suggest alternative mechanisms for virus dissemination such as cell-to-cell spread, dendritic cell-mediated transfer, and cytokine-augmented dispersal of progeny virions all may contribute to this process. The extremely-rapid systemic spread exhibited by SIV and SHIVs in macaques and presumably, by HIV-1 in humans, during the acute infection clearly requires prompt, potent, and sustained interventions to prevent the establishment of a chronic infection and an otherwise fatal clinical outcome. The rapid pace of virus dissemination presents a formidable challenge for the development of an effective prophylactic HIV vaccine.

Methods

Virus and Animals. The origin and preparation of the tissue culture-derived $SHIV_{DH12R}$ and molecular clone-derived SIV_{mac239} stocks have been described (36). Rhesus macaques (*Macaca mulatta*) were maintained in accordance with the guidelines of the Committee on Care and Use of Laboratory Animals and were housed in a biosafety level 2 facility; biosafety level 3 practices were followed (36).

Plasma Viral RNA Quantitation. Viral RNA levels in plasma were determined by real-time RT-PCR (ABI Prism 7700 Sequence Detection System; Applied Biosystems) as described (20).

Lymphocyte Immunophenotyping and Live Cell Sorting. EDTA-treated blood samples were stained for flow cytometric analysis as described (20). The preparation of positively-sorted naïve and memory CD4+ T cells negatively sorted resting and CD4+ T cells are described in *SI Text*. The purity of the resulting CD4+ T cell populations, negative for non-CD4 and activation markers (CD25, CD69, and HLA-DR), from both animals was >96%.

Calibration of Cell Numbers for Quantitative DNA and Alu-LTR PCR. Cell numbers in each genomic DNA sample were determined by quantitative PCR of albumin genes, by using an ABI Prism 7700 Sequence Detection System. The rhesus macaque albumin primer and probe sequences were AlbF, TGCATGAGAAAACGCCAGTAA; AlbR, ATGGTCGCCTGTTCACCAA; and AlbP, AGAAAGTCACCAAATGCTGCACGGAATC, as described (20). The standard used was rhesus macaque genomic DNA present in known numbers of PBMCs, as determined by serial limiting dilution.

Cell-Associated DNA Levels in Naïve or Memory CD4+ T Lymphocytes. Cell-associated viral DNA was measured by a quantitative PCR assay for SIV *gag* by using a ABI Prism 7700 Detection System as described (20). Cell numbers

analyzed in each reaction had been determined by quantitative PCR of albumin DNA in each sample.

Resting CD4+ T Lymphocytes Culture and Amplification of Infectious Virus in Cultured T Cell Lines. Negatively-sorted resting CD4+ T cells (2×10^6 cells), were treated with Pronase (Roche; 20 mg/mL), and cultured for 4 days in the absence of any stimulation in RPMI medium 1640 supplemented with 15% autologous serum, collected from each animal before infection. Culture supernatants were assayed for RT activity to measure progeny virus production (21). To amplify progeny virions in supernatants of resting CD4+ T cell cultures, filtered supernatants, collected daily (days 1–4) were spinoculated (37) onto MT-4 T cells in duplicate. Virus production was assessed by measuring the RT activity released into the culture medium on day 14.

Alu-LTR PCR to Detect Integrated Viral DNA. The isolation of a cloned cell line (3D8) containing a single integrated copy of SIV DNA is described in *SI Text*. Genomic DNA was prepared from FACS-sorted naïve and memory CD4+ T cells as described (17). To detect only integrated lentiviral genomes, the described Alu-LTR PCR technique (29) was modified for use with rhesus macaque Alu sequences. To improve the sensitivity of detecting integrated SIV DNA situated near genomic Alu sequences in either orientation, pairs of outward-facing PCR primers, binding to conserved regions of human and rhesus macaque AluDNA sequences were used in combination with an SIV LTR reverse primer, as described (38, 39). For the first-round PCR, genomic DNA was serially diluted in 2-fold dilutions (500 to 2 cell equivalents), and each dilution was divided into triplicate pools. The first-round rhesus Alu -SIV LTR PCR primers were: RS-Alu-1 (+), 5′-TACTCAGGAGGCTGAGGCAGGAG-3′; RS-Alu-2 (−), 5′-GCCTCCCAAAGTACTAGGATTACAG-3′, and SIV2ST3 (−, 5′-CAAACTTCCATGCTAGAACCTCTCCC-3′. The primers used for the nested PCR were SIV.LTR-315–338 (+), 5′-GGAAGAAGGCATCATACCAGATTG-3′ and SIV.LTR.427–448 (−), 5-AATGCTCCTCATCCTCCTGTGC-3′. PCR conditions for both the first-round and nested PCRs have been described (29). SIV LTR nested PCR products were visualized on 2% agarose TAE gels (SeaKem ME Agarose; Cambrex Biosciences) with ethidium bromide (0.5 μg/mL).

ACKNOWLEDGMENTS. We thank Rahel Petros, Joseph Mckennan, Dhirenkumar Patel, and Dr. Boris Skopets for diligently assisting in the care and maintenance of our animals; Robin Kruthers and Ranjini Iyengar for determining viral RNA levels; Charles Buckler for arranging and scheduling animal experiments; and Ronald C. Desrosiers (Harvard Medical School, Boston) for providing molecular clones of SIV_{mac239} and SIV_{mac316}. This work was supported by the Intramural Research Program of the National Institute of Allergy and Infectious Diseases, National Institutes of Health.

1. Zack JA, et al. (1990) HIV-1 entry into quiescent primary lymphocytes: Molecular analysis reveals a labile, latent viral structure. *Cell* 61:213–222.
2. Zagury D, et al. (1986) Long-term cultures of HTLV-III-infected T cells: A model of cytopathology of T cell depletion in AIDS. *Science* 231:850–853.
3. Spina CA, Guatelli JC, Richman DD (1995) Establishment of a stable, inducible form of human immunodeficiency virus type 1 DNA in quiescent CD4 lymphocytes in vitro. *J Virol* 69:2977–2988.
4. Swiggard WJ, O'Doherty U, McGain D, Jeyakumar D, Malim MH (2004) Long HIV type 1 reverse transcripts can accumulate stably within resting CD4+ T cells while short ones are degraded. *AIDS Res Hum Retroviruses* 20:285–295.
5. Zack JA, Haislip AM, Krogstad P, Chen IS (1992) Incompletely reverse-transcribed human immunodeficiency virus type 1 genomes in quiescent cells can function as intermediates in the retroviral life cycle. *J Virol* 66:1717–1725.
6. Bukrinsky MI, et al. (1992) Active nuclear import of human immunodeficiency virus type 1 preintegration complexes. *Proc Natl Acad Sci USA* 89:6580–6584.
7. Sun Y, Clark EA (1999) Expression of the c-myc protooncogene is essential for HIV-1 infection in activated T cells. *J Exp Med* 189:1391–1398.
8. Korin YD, Zack JA (1999) Nonproductive human immunodeficiency virus type 1 infection in nucleoside-treated G_0 lymphocytes. *J Virol* 73:6526–6532.
9. Pierson T, McArthur J, Siliciano RF (2000) Reservoirs for HIV-1: Mechanisms for viral persistence in the presence of antiviral immune responses and antiretroviral therapy. *Annu Rev Immunol* 18:665–708.
10. Brussel A, Sonigo P (2004) Evidence for gene expression by unintegrated human immunodeficiency virus type 1 DNA species. *J Virol* 78:11263–11271.
11. Nakajima N, Lu R, Engelman A (2001) Human immunodeficiency virus type 1 replication in the absence of integrase-mediated DNA recombination: Definition of permissive and nonpermissive T cell lines. *J Virol* 75:7944–7955.
12. Wu Y, Marsh JW (2001) Selective transcription and modulation of resting T cell activity by preintegrated HIV DNA. *Science* 293:1503–1506.
13. Korin YD, Zack JA (1998) Progression to the G_1b phase of the cell cycle is required for completion of human immunodeficiency virus type 1 reverse transcription in T cells. *J Virol* 72:3161–3168.
14. Eckstein DA, et al. (2001) HIV-1 actively replicates in naive CD4+ T cells residing within human lymphoid tissues. *Immunity* 15:671–682.
15. Kinter A, Moorthy A, Jackson R, Fauci AS (2003) Productive HIV infection of resting CD4+ T cells: Role of lymphoid tissue microenvironment and effect of immunomodulating agents. *AIDS Res Hum Retroviruses* 19:847–856.
16. Zhang Z, et al. (1999) Sexual transmission and propagation of SIV and HIV in resting and activated CD4+ T cells. *Science* 286:1353–1357.
17. Nishimura Y, et al. (2005) Resting naive CD4+ T cells are massively infected and eliminated by X4-tropic simian–human immunodeficiency viruses in macaques. *Proc Natl Acad Sci USA* 102:8000–8005.
18. Douek DC, Picker LJ, Koup RA (2003) T cell dynamics in HIV-1 infection. *Annu Rev Immunol* 21:265–304.
19. Grivel JC, Margolis LB (1999) CCR5- and CXCR4-tropic HIV-1 are equally cytopathic for their T cell targets in human lymphoid tissue. *Nat Med* 5:344–346.
20. Nishimura Y, et al. (2004) Highly pathogenic SHIVs and SIVs target different CD4+ T cell subsets in rhesus monkeys, explaining their divergent clinical courses. *Proc Natl Acad Sci USA* 101:12324–12329.
21. Willey RL, et al. (1988) In vitro mutagenesis identifies a region within the envelope gene of the human immunodeficiency virus that is critical for infectivity. *J Virol* 62:139–147.
22. Folks TM, et al. (1989) Tumor necrosis factor α induces expression of human immunodeficiency virus in a chronically infected T cell clone. *Proc Natl Acad Sci USA* 86:2365–2368.
23. Agosto LM, et al. (2007) HIV-1 integrates into resting CD4+ T cells even at low inoculums as demonstrated with an improved assay for HIV-1 integration. *Virology* 368:60–72.
24. Swiggard WJ, et al. (2005) Human immunodeficiency virus type 1 can establish latent infection in resting CD4+ T cells in the absence of activating stimuli. *J Virol* 79:14179–14188.
25. Vatakis DN, Bristol G, Wilkinson TA, Chow SA, Zack JA (2007) Immediate activation fails to rescue efficient human immunodeficiency virus replication in quiescent CD4+ T cells. *J Virol* 81:3574–3582.
26. Li Q, et al. (2005) Peak SIV replication in resting memory CD4+ T cells depletes gut lamina propria CD4+ T cells. *Nature* 434:1148–1152.
27. Blaak H, et al. (2000) In vivo HIV-1 infection of CD45RA+CD4+ T cells is established primarily by syncytium-inducing variants and correlates with the rate of CD4+ T cell decline. *Proc Natl Acad Sci USA* 97:1269–1274.
28. Ostrowski MA, et al. (1999) Both memory and CD45RA+/CD62L+ naive CD4+ T cells are infected in human immunodeficiency virus type 1-infected individuals. *J Virol* 73:6430–6435.
29. Chun TW, et al. (1997) Presence of an inducible HIV-1 latent reservoir during highly active antiretroviral therapy. *Proc Natl Acad Sci USA* 94:13193–13197.
30. Finzi D, et al. (1997) Identification of a reservoir for HIV-1 in patients on highly active antiretroviral therapy. *Science* 278:1295–1300.
31. Wong JK, et al. (1997) Recovery of replication-competent HIV despite prolonged suppression of plasma viremia. *Science* 278:1291–1295.
32. Chun TW, et al. (2003) Gene expression and viral prodution in latently infected, resting CD4+ T cells in viremic versus aviremic HIV-infected individuals. *Proc Natl Acad Sci USA* 100:1908–1913.
33. Chun TW, et al. (1997) Quantification of latent tissue reservoirs and total body viral load in HIV-1 infection. *Nature* 387:183–188.
34. Mattapallil JJ, et al. (2005) Massive infection and loss of memory CD4+ T cells in multiple tissues during acute SIV infection. *Nature* 434:1093–1097.
35. Reilly C, Wietgrefe S, Sedgewick G, Haase A (2007) Determination of simian immunodeficiency virus production by infected activated and resting cells. *AIDS* 21:163–168.
36. Igarashi T, et al. (1999) Emergence of a highly pathogenic simian/human immunodeficiency virus in a rhesus macaque treated with anti-CD8 mAb during a primary infection with a nonpathogenic virus. *Proc Natl Acad Sci USA* 96:14049–14054.
37. O'Doherty U, Swiggard WJ, Malim MH (2000) Human immunodeficiency virus type 1 spinoculation enhances infection through virus binding. *J Virol* 74:10074–10080.
38. Brussel A, Sonigo P (2003) Analysis of early human immunodeficiency virus type 1 DNA synthesis by use of a new sensitive assay for quantifying integrated provirus. *J Virol* 77:10119–10124.
39. Sonza S, et al. (1996) Human immunodeficiency virus type 1 replication is blocked prior to reverse transcription and integration in freshly isolated peripheral blood monocytes. *J Virol* 70:3863–3869.

JOURNAL OF VIROLOGY, July 2009, p. 7099–7108
0022-538X/09/$08.00+0 doi:10.1128/JVI.02522-08

Vol. 83, No. 14

Initiation of Antiretroviral Therapy 48 Hours after Infection with Simian Immunodeficiency Virus Potently Suppresses Acute-Phase Viremia and Blocks the Massive Loss of Memory CD4$^+$ T Cells but Fails To Prevent Disease$^\nabla$

Makoto Kubo,† Yoshiaki Nishimura, Masashi Shingai, Wendy Lee, Jason Brenchley, Bernard Lafont, Alicia Buckler-White, Tatsuhiko Igarashi, and Malcolm A. Martin*

Laboratory of Molecular Microbiology, National Institute of Allergy and Infectious Diseases, National Institutes of Health, Bethesda, Maryland 20892

Received 8 December 2008/Accepted 29 April 2009

We investigated whether a 28-day course of potent antiretroviral therapy, initiated at a time point (48 h postinoculation) following simian immunodeficiency virus (SIV) inoculation when the acquisition of a viral infection was virtually assured, would sufficiently sensitize the immune system and result in controlled virus replication when treatment was stopped. The administration of tenofovir 48 h after SIV inoculation to six *Mamu-A*01*-negative rhesus macaques did, in fact, potently suppress virus replication in all of the treated rhesus macaques, but plasma viral RNA rapidly became detectable in all six animals following its cessation. Unexpectedly, the viral set points in the treated monkeys became established at two distinct levels. Three controller macaques had chronic phase virus loads in the range of 1×10^3 RNA copies/ml, whereas three noncontroller animals had set points of 2×10^5 to 8×10^5 RNA copies/ml. All of the noncontroller monkeys died with symptoms of immunodeficiency by week 60 postinfection, whereas two of the three controller animals were alive at week 80. Interestingly, the three controller macaques each carried major histocompatibility complex class I alleles that previously were reported to confer protection against SIV, and two of these animals generated cytotoxic T-lymphocyte escape viral variants during the course of their infections.

Acute human immunodeficiency virus (HIV) and simian immunodeficiency virus (SIV) infections are characterized by the extensive and rapid killing of memory CD4$^+$ T lymphocytes at multiple effector sites, including the gastrointestinal tract (1, 5, 10, 17, 18, 31). Previous studies have utilized transient early postinoculation antiretroviral therapy (ART) to blunt the acute infection and to preserve the integrity of the immune system. Initiating a 28-day course of the reverse transcriptase (RT) inhibitor tenofovir (PMPA) at 24 h post inoculation (p.i.) of rhesus macaques with either SIVmac239 or SIVsmE660 potently suppressed virus replication during and following drug administration (11, 12). In contrast, extending the time of treatment start from 24 to 72 h after SIVsmE660 infection resulted in two of four animals becoming viremic during the 28-day course of therapy and generating measurable levels of plasma viral RNA in all four monkeys following the cessation of ART (12).

Based on these reports, which suggested that ART started at 24 h potently aborted the SIV infection, we elected to delay the treatment after virus inoculation until 48 h p.i. to permit a controlled establishment of the viral infection and possibly enable a sensitized immune system to control virus replication when PMPA treatment was discontinued. Accordingly, we treated six *Mamu-A*01*-negative Indian-origin rhesus macaques with the RT inhibitor beginning at 48 h p.i. Although virus replication (monitored by RT-PCR and cell-associated DNA PCR) was effectively suppressed and memory CD4$^+$ T cells in the blood and at an effector site (lung) were preserved, plasma viremia became detectable in all six of the treated animals immediately following the cessation of ART. Interestingly, by 15 weeks p.i., the plasma viral RNA set points of the treated monkeys had become established at two distinct levels. Three animals (termed noncontrollers) had plasma viral RNA loads in the range of 10^5 to 10^6 viral RNA copies/ml (similar to untreated SIV-inoculated macaques), and three monkeys (termed controllers) had viral loads in the range of 10^3 viral RNA copies/ml. Analyses of the major histocompatibility complex (MHC) class I alleles in the tenofovir-treated cohort revealed that the three controllers carried genes (*Mamu-B*08*, *Mamu-B*29*, and *Mamu-A*02*) previously associated with the suppression of virus replication in SIV-inoculated rhesus macaques (15, 20, 25). Nevertheless, two of the controller macaques began to experience the loss of memory CD4$^+$ T cells at months 9 and 11 postchallenge, respectively. This was accompanied by marked increases in the levels of their set point viremia, from approximately 10^3 RNA copies/ml to 10^5 to 10^6 RNA copies/ml. Changes in immunodominant restricting CD8$^+$ T-cell epitopes were observed in two of the controller macaques. At week 80 p.i., only two tenofovir-treated animals, both bearing protective MHC alleles, remained alive.

* Corresponding author. Mailing address: Bldg. 4, Rm. 315A, 4 Center Dr. MSC 0460, National Institutes of Health, Bethesda, MD 20892-0460. Phone: (301) 496-4012. Fax: (301) 402-0226. E-mail: malm@nih.gov.

† Present address: Division of Immunology, Kitasato University of Allied Health Sciences, 1-15-1 Kitasata Sagamihara, Kanagawa 228-8555, Japan.

$^\nabla$ Published ahead of print on 6 May 2009.

MATERIALS AND METHODS

Virus and animal experiments. The origin and preparation of the tissue culture-derived SIVmac239 stocks from molecular clones have been described previously (7, 21). Adult rhesus macaques (*Macaca mulatta*), weighing between 4.7 and 6.2 kg, were maintained in accordance with the guidelines of the Committee on Care and Use of Laboratory Animals (3) and were housed in a biosafety level 2 facility; biosafety level 3 practices were followed. All rhesus macaques were *Mamu-A*01* negative.

Tenofovir treatment of SIVmac239-infected rhesus macaques. Tenofovir {9-[2-(*R*)-(phosphonometoxy)propyl]adenine} was generously provided by Norbert Bischofberger, Gilead Science, Inc. (Foster City, CA). An aqueous solution (200 mg/ml) of PMPA was prepared after adjusting the pH to 7.0 with NaOH and filtration through a membrane filter (pore size, 0.22 μm) as previously described (30). Tenofovir was intramuscularly administered (30 mg/kg of body weight) every 24 h for 4 weeks, starting at 48 h p.i. with 100 50% tissue culture infectious doses ($TCID_{50}$) of SIVmac239.

Quantitation of proviral DNA and plasma viral RNA levels. The number of viral DNA copies in peripheral blood mononuclear cells was measured by quantitative DNA PCR (29). Viral RNA levels in plasma were determined by real-time reverse transcription-PCR (ABI Prism 7700 sequence detection system; Applied Biosystems, Foster City, CA) as previously reported, using reverse-transcribed viral RNA in plasma samples from SIVmac239-inoculated rhesus macaques (4).

Amplification of viral RNA to identify SIV escape variants. To analyze SIV variants bearing mutations affecting epitopes restricted by MHC class I alleles, plasma viral RNA was extracted using a QIAamp viral RNA mini-kit (Qiagen) and then reverse transcribed using SuperScript III First-Strand Synthesis SuperMix (Invitrogen). PCR amplifications were performed using primer sets SIVmac239(1407-1436)-F (TGTAGTATGGGCAGCAAATGAATTAGATAG) and SIVmac239 (2701-2681)-R (GGTCCTCTGGGGGAGCAGTTG) for the GY9 Mamu-A*02 epitope, SIVmac239(5093-5116)-F (ATTGGCAGGCAGATGGCCTATTAC) and SIVmac239(6454-6431)-R (CCATGGTTCCCTTTGTGGTCCTTC) for the RL8 and RL9 Mamu-B*08 epitopes, SIVmac239(7005-7027)-F (GGGATACTTGGGG AACAACTCAG) and SIVmac239(9380-9358)-R (CAGATCTCCAGACGGCCT GGACC) for the RY8 Mamu-A*02 epitope, SIVmac239(9381-9405)-F (CGACA GAGACTCTTGCGGGCGCGTG) and SIVmac239(10129-10104)-R (CTGTTTC AGCGAGTTTCCTTCTTGTC) for YY9 of the Mamu-A*02 epitope, and the RL9 and RL10 Mamu-B*08 epitopes. The PCRs were performed using 10 pmol of each forward and reverse primer, Platinum PCR SuperMix High Fidelity (Invitrogen), and 1 μl of viral cDNA in a final volume of 50 μl. The reaction mixtures were heated to 94°C for 2 min, followed by 32 cycles of denaturing at 94°C for 20 s, annealing at 58°C for 30 s, and extension at 68°C for 2 min. A final extension was conducted at 68°C for 7 min. PCR products were gel extracted using a Qiaquick gel extraction kit (Qiagen), cloned into pCR2.1 TOPO cloning vector (Invitrogen), and then sequenced.

Lymphocyte immunophenotyping in monkey BAL fluid and peripheral blood. Bronchoalveolar lavage (BAL) lymphocytes were prepared from uninfected donor animals and SIV-inoculated animals by using a pediatric bronchoscope (BF3C40; Olympus America, Inc., Melville, NY), as previously described (7). The BAL fluid was filtered through a 70-μm-pore-size cell strainer (BD Falcon, Bedford, MA) and centrifuged, and the cell pellet was washed three times with 1% bovine serum albumin (Sigma-Aldrich, St. Louis, MO)-phosphate buffered saline (1% BSA-PBS). The cells were resuspended in mouse immunoglobulin (Ig) (1 mg/ml)–1% BSA-PBS. EDTA-treated blood samples and cells from BAL specimens were stained for flow-cytometric analysis as described previously (22, 23) using combinations of the following fluorochrome-conjugated monoclonal antibodies (MAbs): CD3 (phycoerythrin [PE]), CD4 (peridinin chlorophyll protein-Cy5.5 [PerCP-Cy5.5]), CD8 (PerCP or allophycocyanin [APC]), CD28 (fluorescein isothiocyanate [FITC] or PE), or CD95 (APC). All antibodies were obtained from BD Biosciences (San Diego, CA), samples were analyzed by four-color flow cytometry (FACSCalibur; BD Biosciences Immunocytometry Systems), and data analysis was performed using CellQuest Pro (BD Biosciences, San Diego, CA). In this study, naïve $CD4^+$ T cells were identified by their $CD95^{low}$ $CD28^{high}$ phenotype, whereas memory $CD4^+$ T cells were $CD95^{high}$ $CD28^{high}$ or $CD95^{high}$ $CD28^{low}$ in the $CD4^+$ small lymphocyte gate (27).

Intracellular cytokine assays. Stimulation was performed on frozen lymphocytes as described previously (28). Freshly thawed lymphocytes were resuspended (10^6/ml) in RPMI medium supplemented with antibiotics and glutamine. Anti-CD28 conjugated to Alexa 594-PE was used for costimulation. *Staphylococcus* enterotoxin B (1 μg/ml; Sigma-Aldrich, St. Louis, MO) was used to stimulate T cells mitogenically through the T-cell receptor as a positive control. A negative control (cells treated only with costimulatory anti-CD28) was included in every experiment. Peptides used to stimulate SIV-specific T cells were 15 amino acids in length, overlapping by 11 amino acids, and encompassed SIVmac239 Gag (New England Peptide, Gardner, MA). The concentration of each peptide was 2 μg/ml for stimulations, which were performed in the presence of brefeldin-A (BFA; 1 μg/ml; Sigma-Aldrich, St. Louis, MO) for 16 h at 37°C. All cells were surface stained with the dead cell exclusion dye Aqua Blue (Invitrogen Corporation, Carlsbad, CA), followed by staining with anti-CD3 Alexa700 (BD), anti-CD4 Cy5.5-PE (eBioscience Inc., San Diego, CA), anti-CD8 Pacific Blue (BD), and anti-CD95 Cy5-PE (BD). Cells then were fixed, permeabilized, stained with anti-gamma interferon (IFN-γ) Cy7-PE (BD), anti-interleukin-2 (IL-2) APC (BD), tumor necrosis factor (TNF) FITC (BD), and Mip1-β PE (BD) and analyzed by flow cytometry (FACSAria; BD Biosciences Immunocytometry Systems). SIV-specific CD8 T-cell responses are reported as the frequency of memory CD8 T cells gated by characteristic light scatter properties, and then as Aqua blue-negative, $CD3^+$, $CD8^+$, $CD4^-$, $CD95^+$, and by the production of either TNF or Mip-1β. All data are reported after background subtraction.

Cells also were purified from freshly collected BAL specimens as described above and resuspended in RPMI 1640 medium (Cambrex Bio Science, Walkersville, MD) supplemented with 10% fetal bovine serum (HyClone, Loagan, UT), 2 mM L-glutamine, 1 mM sodium pyruvate, and 100 U/ml penicillin–0.1 mg/ml streptomycin (Sigma-Aldrich, St. Louis, MO). The cells then were stimulated with the SIVmac239 Gag peptide pool at a concentration of 10 μM. After 2 h of incubation, BFA (Sigma) was added to block protein transport, and following four additional hours of incubation, the cells were stained for flow cytometry using combinations of the following fluorochrome-conjugated MAbs: CD3 (FITC) and CD8 (PerCP). For IFN-γ staining, cells were treated with fluorescence-activated cell sorting permeabilization buffer 2 (Becton Dickinson) and stained with CD69 (PE) and IFN-γ (APC) MAbs. All antibodies were obtained from BD Biosciences (San Diego, CA). IFN-γ production in $CD8^+$ T cells was analyzed with a FACSCalibur. The percentage of IFN-γ-producing memory $CD8^+$ T cells in BAL samples was calculated after subtracting values obtained with contemporaneously analyzed mock-infected cells.

MHC class I cDNA cloning and sequencing. The cloning of Mamu-A and Mamu-B cDNA from rhesus macaques was performed by RT-PCR amplification as described previously (9). Briefly, total cellular RNA was extracted from activated rhesus peripheral blood mononuclear cells using TRI reagent (Molecular Research Center, Cincinnati, OH). Complete Mamu-A and Mamu-B cDNAs were generated using the 3′ rapid amplification of cDNA ends (RACE) adapter from the First Choice RLM RACE kit (Ambion, Austin, TX). PCR amplifications were performed using sense primer Mane5UA (GATTCTCCGCAGACG CCCA), Mane5UA20 (GATTCTCCGCAGACGCCAA), Mane5UB2 (AAAGT CTCCTCAGACGCCGA), or Mane5UB3 (AGAGTCTCCTCAGACCCCAA), oligonucleotides annealing in the 5′-untranslated region of Mamu-A or -B cDNA, and the 3′ RACE outer reverse primer. The PCR mixtures contained 50 mM potassium acetate, 1.5 mM $MgSO_4$, 10 mM Tris-HCl, pH 9.0, 0.2 mM each dGTP, dCTP, dATP, and dTTP, 20 pmol of each sense and reverse primers, and 5 U of Super *Taq* Plus DNA polymerase (Ambion, Austin, TX). Each reaction mixture contained 2 μl of cDNA in a final volume of 50 μl. The reaction mixtures were heated at 95°C for 3 min, and then amplification was conducted for 30 cycles as follows: denatured for 30 s at 95°C, annealed for 30 s at 59°C, and extended for 90 s at 72°C. A final extension was conducted for 7 min at 72°C. PCR products were gel purified using a Qiaquick gel extraction kit (Qiagen, Valencia, CA) and then cloned into pCR2.1 TOPO cloning vector (Invitrogen, Carlsbad, CA). Insert-containing clones were identified after restriction analysis using EcoRI and then were sequenced using an Applied Biosystems 3130XL genetic analyzer.

Sequence analysis and allele identification. Sequences were aligned using the Clustal W program of MacVector 10.0.2 software (MacVector Inc., Cary, NC) with a panel of 56 Mamu-A and 157 Mamu-B published alleles. Phylogenetic trees were constructed based on the alignment using the neighbor-joining method of the software. Genetic distances were estimated using Kimura's two-parameter method. Alleles were identified based on the close clustering of cloned sequences with known alleles.

Western blot analysis. For immunoblotting, SIVmac239 particles were concentrated by ultracentrifugation (100,000 × g for 75 min by using a Type 55 rotor in an Optima XL-100K Ultracentrifuge; Beckman Coulter, Fullerton, CA). The virus pellet was resuspended in PBS and subjected to ultracentrifugation through 20% sucrose in PBS (200,000 × g for 75 min in an SW55 rotor using an Optima XL-100K Ultracentrifuge; Beckman Coulter). After incubation with sodium dodecyl sulfate-polyacrylamide gel electrophoresis (SDS-PAGE) sample buffer, viral proteins were resolved by SDS-PAGE and transferred to a polyvinylidene difluoride membrane (Invitrolon PVDF; Invitrogen, Carlsbad, CA). The membranes were incubated with serially collected plasma samples (diluted 1:500),

TABLE 1. Experimental protocol

Animal	SIVmac239 inoculum size ($TCID_{50}$)	Tenofovir dose (mg/kg/day)	Tenofovir initiation time point (h p.i.)	Tenofovir duration (days)
CL8P	100	30	48	28
DA14	100	30	48	28
DA21	100	30	48	28
DA63	100	30	48	28
DA87	100	30	48	28
DB05	100	30	48	28
CK2G	100	None		
CL33	100	None		

which had been preadsorbed with sonicated lysate of *Escherichia coli* and MT-4 cells, and then with goat anti-monkey IgG conjugated with horseradish peroxidase (Santa Cruz Biotechnology, Santa Cruz, CA). Protein bands were visualized on X-ray film (Kodak Biomax MR) after incubation with chemiluminescent substrate (Western Blotting Luminol Reagent; Santa Cruz Biotechnology, Santa Cruz, CA).

Anti-SIV Env ELISA. Anti-SIV gp130 Env-specific IgGs in monkey plasma were detected and quantified by end point dilution enzyme-linked immunosorbent assay (ELISA). Flat-bottomed 96-well plates (Corning, Lowell, MA) were coated with purified recombinant SIVmac239 gp130 (6) that had been obtained from the NIH AIDS Research and Reference Reagent Program, Division of AIDS, National Institute of Allergy and Infectious Diseases, NIH. The coated plates first were blocked with 4% nonfat milk in PBS and then incubated with serially diluted (in 4% nonfat milk-PBS) samples of macaque plasma (with a starting dilution of 1:100) for 1 h at 37°C, followed by an overnight incubation at 4°C. Horseradish peroxidase-conjugated polyclonal goat anti-monkey IgG (Nordic Immunological Laboratories, The Netherlands) (1:2,000 dilution in 4% nonfat milk-PBS) was used as the secondary antibody. Incubated plates were developed with 2,2′-azino-bis liquid substrate (Sigma-Aldrich, St. Louis, MO), and the endpoint titers, defined as the reciprocal of the highest dilution giving an absorbance reading of more than three times the mean of the preimmune serum at the same dilution, were determined (8).

Virus neutralization assays. Plasma samples (1:20 dilution) from PMPA-treated and untreated SIV-infected macaques were incubated with SIVmac239 in quadruplicate in a total volume of 50 μl for 1 h at 37°C in 96-well flat-bottomed culture plates. Samples from uninfected animals served as controls. Freshly trypsinized TZM-bl cells (33) (1×10^4 in 150 μl Dulbecco's modified essential medium containing 20 μg/ml DEAE dextran) were added to each well, and the cultures were maintained in a 37°C incubator for 28 h. The amount of virus-induced luciferase activity present in cell lysates was determined using a commercially available luciferase assay kit (Invitrogen Corporation, Carlsbad, CA), and the average neutralization activity for each plasma sample was determined. Any sample resulting in a 50% reduction of luciferase activity compared to that obtained with the uninfected control sample was considered positive for neutralizing antibodies (NAbs).

RESULTS

The aim of this study was to administer a proven ART regimen very early during acute SIV infection that would effectively suppress virus replication, and to ascertain whether immune responses would be sufficiently activated during drug administration to control virus replication following treatment cessation. As indicated in Table 1, six *Mamu-A*01*-negative Indian-origin rhesus macaques were inoculated intravenously with 100 $TCID_{50}$ of SIVmac239; treatment with PMPA commenced at 48 h p.i. This time for treatment initiation was selected based on two previous reports: the first showed that tenofovir administration beginning at 24 h p.i. resulted in no measurable plasma viremia during, or 6 weeks following, ART in three of four animals infected with SIVsmE660 (12); and the second showed that treatment initiated 24 h after SIVmac239 inoculation led to low to unmeasurable plasma viral RNA levels during 28 days of PMPA therapy or for an additional 6 weeks following the discontinuation of ART (11). When tenofovir treatment was delayed until 72 h p.i., SIVsmE660 viremia was detectable during the 4-week course of therapy in two of four monkeys and in four of four animals following the cessation of drug administration (12). Thus, the start of ART at 48 h p.i. would ensure SIV acquisition and the possible stimulation of the immune system while limiting injury to the $CD4^+$ T-cell population. Two age-matched untreated but SIV-infected macaques served as controls (Table 1).

PMPA potently suppresses virus replication during acute SIV infection. As expected, the two untreated animals inoculated with 100 $TCID_{50}$ SIVmac239 developed peak levels of plasma viremia (5.6×10^6 and 7.1×10^6 RNA copies/ml, respectively) and high frequencies of cell-associated viral DNA on day 14 p.i. (Fig. 1). In contrast, no plasma viral RNA was measurable in four of the six tenofovir-treated macaques (the limit of detection is 100 viral RNA copies/ml) during the 4-week course of antiretroviral administration. One treated monkey (DA87) had detectable SIV RNA in its plasma on days 3 (4.3×10^2 copies/ml) and 7 (1.8×10^3 copies/ml) p.i. and none thereafter; a second (DA21) had persistent low levels of viremia (730 to 4,600 RNA copies/ml) throughout the period of tenofovir administration. The level of cell-associated viral DNA was below the threshold of detection in all six of the SIV-infected and PMPA-treated monkeys (the limit of detection is 1 infected cell per 10^6 cells). Taken together, these results indicate that the p.i. ART was highly effective; plasma viremia during the first 4 weeks after SIV inoculation had been

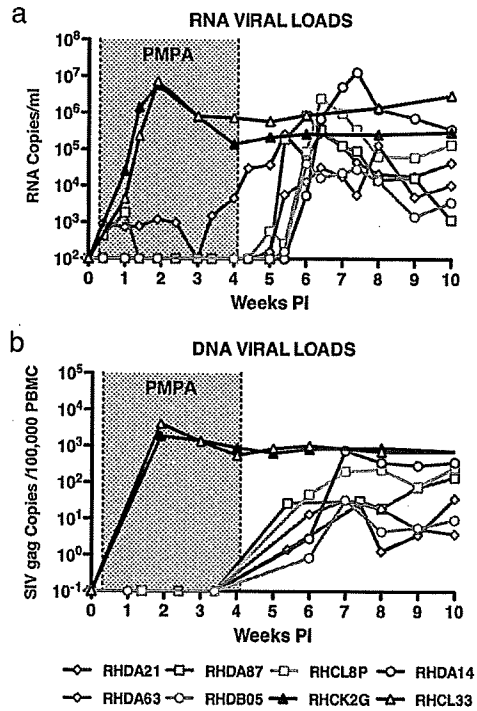

FIG. 1. Plasma viral RNA and cell-associated DNA levels during acute SIV infections. Sequential viral RNA (a) and DNA (b) loads are shown. Tenofovir-treated and untreated animals are indicated in Table 1.

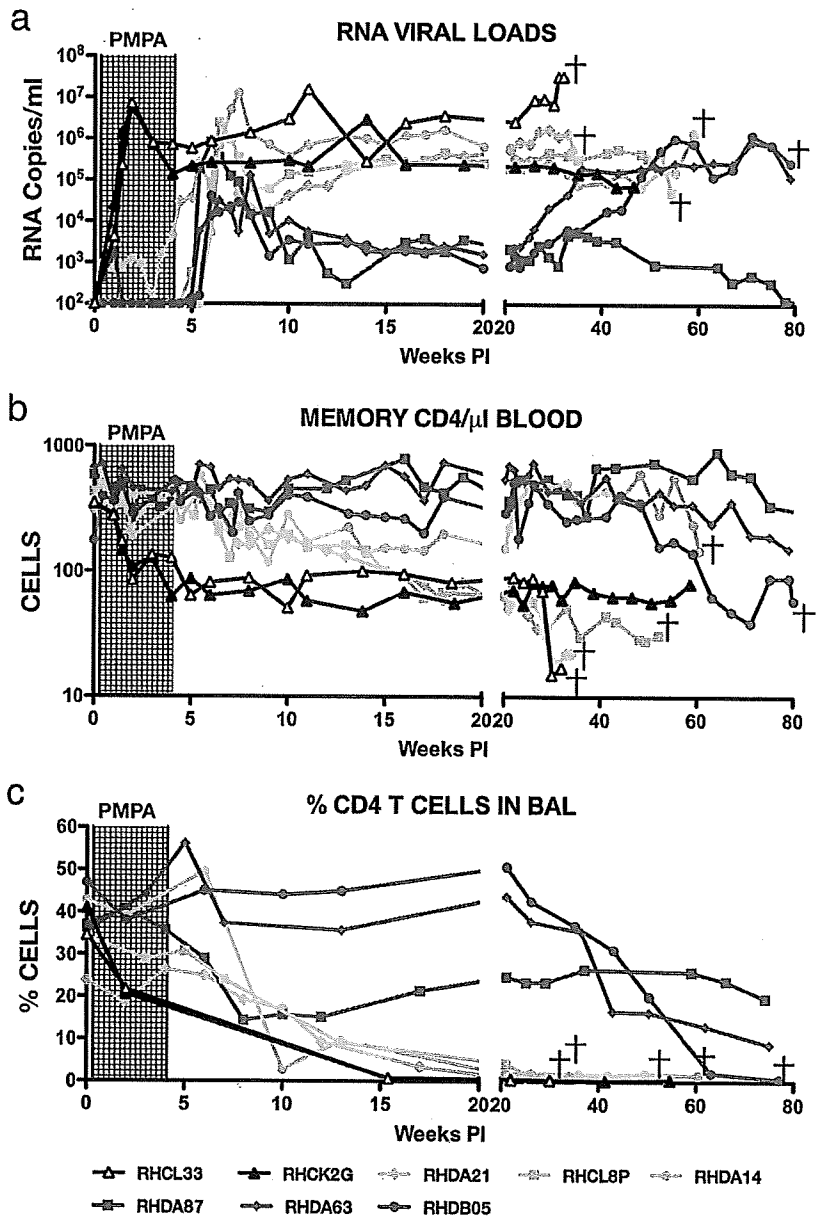

FIG. 2. SIV controller and noncontroller animals establish two distinct levels of set point viremia. Levels of plasma viral RNA (a) and circulating memory $CD4^+$ T cells (b) and the percentage of $CD4^+$ T cells in BAL specimens (c) during the 80 weeks of SIV infection are shown. Controller (red), noncontroller (blue), and untreated (black) monkeys are indicated.

reduced at least 3 to 4 logs in the cohort of treated infected macaques.

Within 7 to 14 days of stopping PMPA therapy, however, SIV replication became detectable in all of the treated monkeys (Fig. 1a). The levels of peak plasma viremia ranged from 3.2×10^4 to 1.3×10^7 RNA copies/ml, with a geometric mean (6.7×10^5) that was approximately 10-fold lower than that observed in the untreated control macaques 4 to 5 weeks earlier. Cell-associated viral DNA, which was not detected during tenofovir administration in any of the treated monkeys, became measurable only after the cessation of ART (Fig. 1b). The two treated animals (CL8P and DA14) with the highest levels of peak plasma viremia also had the highest levels of cell-associated viral DNA.

Viral set points in PMPA-treated monkeys were established at two distinct levels. The six recipients of tenofovir resolved their acute SIV infections by week 15 p.i. (Fig. 2a). Interestingly, three of these monkeys (DA87, DA63, and DB05) controlled their plasma viral loads to relatively low levels, whereas the other three drug-treated macaques (DA21, CL8P, and DA14) had viral set points that were several hundredfold higher. At week 22 p.i., the geometric mean plasma virus load for the three controller animals was 1.33×10^3 RNA copies/ml. In contrast, the comparable set point value for the three noncontroller monkeys was 3.6×10^5